ORIGINS AND DISTRIBUTION OF CHONDRITIC OLIVINE INFERRED FROM WILD 2 AND CHONDRITE MATRIX. D. R. Frank[1], M. E. Zolensky[2], and L. Le[1], [1]JETS/NASA Johnson Space Center, Houston, TX, USA, david.r.frank@nasa.gov, [2]ARES/NASA Johnson Space Center, Houston, TX, USA.

Introduction: To date, only 180 particle impact tracks from Wild 2 have been extracted from the Stardust aerogel collector and even fewer have been thoroughly characterized. In order to provide a cohesive compositional dataset that can be compared to the meteorite record, we have made both major and minor element analyses (TEM/EDXS) of olivine and low-Ca pyroxene for 39 particles harvested from 26 tracks. However, the dearth of equivalent analyses for these phases in chondrite matrix hinders their comparison to the Wild 2 samples. To properly permit comparison of chondritic olivine and pyroxene to the Wild 2 samples, we have also provided a large, comprehensive EPMA dataset (>10^3 analyses) of analogous grains (5-30μm) isolated in L/LL3.0-4, CI, CM, CR, CH, CO, CV, Acfer 094, EH3, EL6, and Kakangari matrix.

Fa Content: Combining our Wild 2 olivine analyses with those available in the literature, we constructed a distribution of fayalite content from 68 representative analyses of 36 particles and 26 tracks [1]. This Wild 2 distribution is entirely lacking a pronounced forsteritic frequency peak that exemplifies the distributions for chondrites (except CVs) (Fig. 1). This distribution is, however, similar to that reported for anhydrous IDPs [2]. We use the bi-modal distributions observed for carbonaceous chondrites (CCs) to define three olivine types:

FeO-rich Olivine ($Fa_{>\sim15}$). Based on Mn/Fe trends and CaO content, we have inferred that most (if not all) of the FeO-rich isolated matrix grains (IMGs) we examined in CM, CO, Acfer 094, CR, CV_{red}, and L/LL chondrites share a common igneous origin with type II chondrules [1,3]. The Mn/Fe ratios of FeO-rich olivine in the Stardust samples imply that this component of Wild 2 is primarily a mixture of type II chondrule fragments and/or microchondrules that were transported from various CC and ordinary chondrite-forming regions.

Forsteritic Olivine (Fa_{0-6}). The forsteritic olivine in matrix appears to originate from multiple sources. Many of the IMGs are compositionally indistinguishable from type I chondrules and a common origin is inferred. However, some IMGs have CaO and Al_2O_3 contents that are inconsistent with type I chondrules, but consistent with AOAs. In particular, forsterite with CaO < ~0.15 is not generally found in CC chondrules, but is common in AOAs [4-7]. Other notable matrix compositions include low-iron Mn-enriched (LIME) olivines and other forsterite grains that are MnO-enriched (> ~0.6 wt.%) relative to type I chondrules. Both AOA and LIME-like compositions are found in CI, CM, CO, Acfer 094, and CR matrix. Thus, it should be no surprise that the fayalite distributions (Fig. 1) for these chondrites have the sharpest forsteritic frequency peaks. Presumably, these peaks represent the sum of type I chondrule fragments, AOA-derived matrix grains, and primitive nebular condensates that accreted directly into matrix. In contrast, the six tracks we examined that had forsteritic olivine are compositionally dissimilar to common IMGs and type I chondrules (Fig. 2).

AOA-like forsterite. Three tracks (57, 111, and 112) had CaO-poor (< ~0.07 wt.%) forsteritic olivine. This composition is inconsistent with type I chondrule olivine but typical of AOA forsterite. Previously, the forsteritic olivine in tracks 57 and 112 was found to be ^{16}O-rich, and a common origin with AOAs was suggested [8,9].

Refractory forsterite. We located one refractory forsterite (FeO < 1.0 wt.%) grain in the terminal particle of track 154 with FeO = 0.41, CaO = 0.25, and Al_2O_3 = 0.51. Cr_2O_3 and MnO were below detection limits (< ~0.07 wt.%). This is relatively high in CaO, high in Al_2O_3, and very low in MnO, a composition that is typical of (both CC and UOC) refractory forsterite in type IA chondrules, the cores of IMGs, and as relict grains in type II chondrules [10]. The forsterite grain we analyzed in the terminal particle of track 130 is compositionally distinct. It is CaO and Al_2O_3 enriched (0.73 and 0.83 wt.%, respectively) with respect to IMGs, type I chondrules, and AOAs (Fig. 2). It is also the only Wild 2 olivine for which we detected Ti (~0.08 wt.% TiO_2). Cr_2O_3 content is near the middle of the range for CC forsterite (0.53 wt.%), but MnO was not detected. These minor element abundances are also similar to refractory forsterite, but there is higher FeO content (2.4 wt.%) in the track 130 olivine.

Relict Grains: Some FeO-rich relict olivine is identified by its high MnO content with respect to type II chondrule olivine. [11] identified one such relict within a type II chondrule in Kainsaz (CO3.2) and noted its compositional similarity to olivine in a chondrule-like particle described by [12] in track 35. We have also identified similar MnO- and FeO-rich olivine within an Efremovka (CV_{red}) chondrule, an IMG in Krymka (LL3.2), an IMG in Bells (CM), and a second

Wild 2 track (track 69). This strongly suggests that the source material was widely distributed across the solar system, but must have been very diluted in the asteroid belt and rather abundant in the Kuiper Belt.

Unique Wild 2 Olivine: The track 26 terminal particle harbors the only Wild 2 olivine studied to date that has no known compositional analogy in the meteorite record (nearly pure fayalite with up to 5.1 wt.% MnO). Other reports of MnO-enriched fayalite in ordinary and CV chondrites have MnO content < 1.9 wt.% [13-15]. Equilibrium thermodynamic models [16] demonstrate that pure fayalite generally forms at lower temperatures, higher water/rock ratios, and at higher pressure than more MgO-rich olivine. [16] also propose a single process to explain the formation of fayalite/silica assemblages in chondrites: aqueous dissolution of amorphous silicate and kamacite, followed by precipitation of silica and fayalite. Since this particle's fayalite coexists with trydimite [17], hydrothermal deposition of this assemblage appears to be the most likely scenario, and the extremely high MnO content may be a signature of the presumed precursor amoprhous silicate that is unique to Wild 2.

Conclusions: [18] hypothesized that *"Wild 2 rocky components are a sample of a ubiquitously distributed flow of nebular solids…"* and may be a fairly representative sampling of most (or even all) regions that produced early nebular solids. Our investigation of Wild 2 and chondritic olivine compositions certainly supports this, demonstrating that the vast majority of the Wild 2 olivine does likely have a common origin with a multitude of chondrite parent bodies. However, it remains unclear whether Wild 2 accreted material from every chondrite-forming region. In particular, $Fa_{45\text{-}70}$ is relatively abundant within both type II chondrules and IMGs in CM and CO chondrites, but there is only one occurrence of this so far in Wild 2 terminal particles. We certainly require many more Wild 2 olivine analyses to more accurately define its true compositional range, but our current data suggests that CM and CO material may be rather diluted in Wild 2, while CR, CH, and UOC material may be rather abundant. In a general sense, we propose that this flow was dominated by ^{16}O-rich, refractory and AOA-like forsteritic olivine, rare relict grain compositions, and type II chondrule fragments. The paucity of type I chondrule olivine naturally yields the flat distribution of fayalite contents. Therefore, we infer that radial transport of both ^{16}O-rich forsterite and type II chondrule olivine was efficient, but transport of type I chondrule olivine was relatively inefficient. If ^{16}O-rich olivine formed prior to typical type I chondrules, then the efficiency of outward transport to the Kuiper Belt may have been episodic.

References: [1] Frank D. R. et al. *GCA, forthcoming*. [2] Zolensky and Barrett (1994) *MAPS, 29*, 616-620. [3] Frank D. R. et al. (2012) *LPS XLIII*, Abstract #2748. [4] Chizmadia et al. (2002) *MAPS, 37*, 1781-1796. [5] Weisberg et al. (2004) *MAPS, 39*, 1741-1753. [6] Krot et al. (2004) *Chemie der Erde, 64*, 185-239. [7] Sugiura et al. (2009) *MAPS, 44*, 559-572. [8] Nakamura-Messenger K. et al. (2011) *MAPS, 46*, 1033-1051. [9] Nakashima D. et al. (2012) *EPSL, 357-358*, 355-365. [10] Steele I. M. (1986) *GCA, 50*, 1379-1395. [11] Berlin et al. (2011) *MAPS, 46*, 513-533. [12] Nakamura et al. (2008) *Science, 321*, 1664. [13] Brigham et al. (1986) *GCA, 50*, 1655-1666. [14] Wasson and Krot (1994) *EPSL, 122*, 403-416. [15] Hua and Buseck (1995) *GCA, 59*, 563-578. [16] Zolotov et al. (2006) *MAPS, 41*, 1775-1796. [17] Joswiak et al. (2012) *MAPS, 47*, 471-524. [18] Brownlee D. et al. (2012) *MAPS, 47*, 453-470. [19] Steele I. M. (1990) *MAPS, 25*, 301-307.

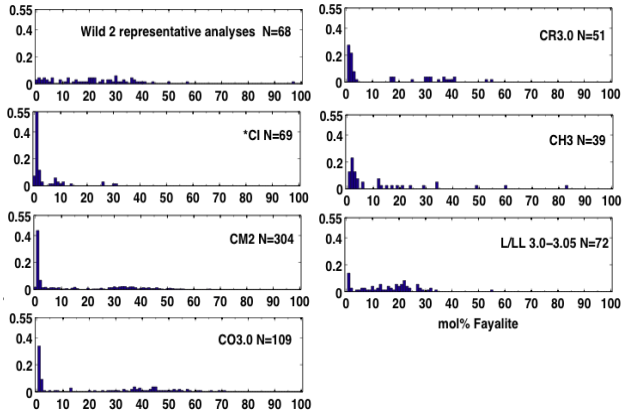

Figure 1: Distributions of fayalite content in Wild 2 and IMGs. *Includes analyses by us and [19].

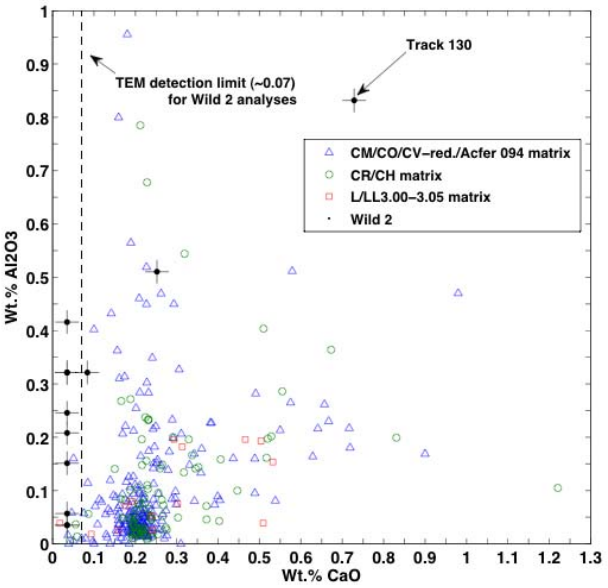

Figure 2: CaO vs. Al_2O_3 for the forsteritic olivine ($Fa_{0\text{-}6}$) in Wild 2 and IMGs.